



REGULAR ARTICLE

Influence of Electrochemical Nickelizing on the Structure, Composition, and Heat Resistance of AISI 1045 after Chromoaluminizing

T. Loskutova<sup>1,2</sup>, Ya. Kononenko<sup>1</sup>, N. Kharchenko<sup>3</sup>, O. Umanskyi<sup>4</sup>, D. Vedel<sup>4</sup>, T. Hovorun<sup>3,\*</sup>

<sup>1</sup> National Technical University of Ukraine "I. Sikorsky Kyiv Polytechnic Institute", 03056 Kyiv, Ukraine

<sup>2</sup> Otto-von-Guericke University Magdeburg, 39106 Magdeburg, Germany

<sup>3</sup> Sumy State University, 40007 Sumy, Ukraine

<sup>4</sup> Frantsevich Institute for Problems of Materials Science, National Academy of Science of Ukraine, 03142 Kyiv, Ukraine

(Received 10 January 2025; revised manuscript received 15 February 2025; published online 27 February 2025)

The processes of forming diffusion coatings on AISI 1045 steel were studied after two saturation methods: diffusion chromoaluminizing and a complex two-stage treatment (electrochemical nickel plating followed by diffusion chromoaluminizing). Nickel plating was performed in nickel sulfate-based electrolytes at a temperature of 40 °C and a current density of 3 A/dm<sup>2</sup>. Complex chromoaluminizing was conducted using a powder method at 1050 °C for 4 hours. It was found that diffusion coatings with a total thickness of 20.5 μm to 23.0 μm were formed on the surface, along with a transition zone based on the α-Fe solid solution with a thickness of up to 55 μm. Micro-X-ray spectral analysis revealed the presence of chromium nitride Cr<sub>2</sub>N, as well as zones with Cr<sub>2</sub>Al phases and a solid solution of chromium and aluminum. The obtained coating consists of four distinct zones, and the surface layer's microhardness was in the range of 16.0 to 16.2 GPa. Diffusion chromoaluminizing of steel 45 samples with a nickel-based layer 20 μm thick was carried out at 1050 °C for 4 hours. The complex two-stage treatment resulted in the formation of a coating with a thickness of 35 to 45 μm. It was demonstrated that the formation of protective coatings significantly improves the oxidation resistance of steel 45 due to the development of a dense oxide film. The structure of oxide inclusions, which contain chromium, aluminum, and iron forming spinel phases, was identified. The two-stage process with preliminary nickel plating ensured a uniform distribution of heterogeneous layers without delamination. Additionally, preliminary nickel plating altered the oxidation mechanism and allowed for coatings with increased plasticity.

**Keywords:** Coating, Complex diffusion saturation, Oxide.

DOI: [10.21272/jnep.17\(1\).01024](https://doi.org/10.21272/jnep.17(1).01024)

PACS numbers: 81.10. – h, 81.10.Dn,  
61.43.Bn, 61.50.Ks, 81.30.Hd

## 1. INTRODUCTION

An intensive search for new methods and technologies for modifying the surface layers of metals and alloys is conducted in modern literature [1-5]. The use of complex alloys is, in most cases, impractical, economically and technologically unjustified, since the surface layer of the material is primarily responsible for most operational characteristics. By changing the structure, phase, and chemical composition of the material's surface through the formation of protective coatings, it is possible to significantly improve its operational properties, such as hardness, strength, wear resistance, heat resistance, corrosion resistance, and others. A gradient structure is formed on the products, which combines the necessary high surface properties with the required base properties. The most common methods involve using coatings obtained through chemical-thermal treatment or electrolytic deposition.

It is known that the formation of diffusion layers on the surface of metals and alloys based on elements with a high affinity for oxygen, such as Cr and Al, contributes to improving heat resistance. These elements tend to form continuous protective films based on Cr<sub>2</sub>O<sub>3</sub> and Al<sub>2</sub>O<sub>3</sub> [6-8]. However, these elements are ferrite-stabilizing and may cause the formation of a transition zone under the coating based on solid solutions in α-Fe(Al, Cr) [9]. The undesirable diffusion redistribution of elements between the coating and the substrate, as well as between the substrate and the external contact environment, can be prevented by using barrier layers.

Barrier coatings based on carbides [10, 11], nitrides [12], borides [13], silicides of transition metals, aluminum oxides, and yttrium oxides [14-16] have found widespread application. Electrochemical nickel plating is extensively used in industry as a barrier coating that impedes metal diffusion [17]. In work [18], the positive effect of an electrochemically nickel-based layer as a barrier was noted. It slows down the

\* Correspondence e-mail: [hovorun@pmtkm.sumdu.edu.ua](mailto:hovorun@pmtkm.sumdu.edu.ua)



degradation process of the aluminized layer on AISI 1045 steel at high temperatures. Degradation and dissolution of the aluminized layer are accompanied by a decrease in its microhardness, particularly intensively in the surface layers of the coating. Higher stability of coatings obtained through aluminizing in the presence of a nickel barrier layer is primarily associated with the formation of ordered compounds in the diffusion layer, which inhibit diffusion processes.

Diffusion chromoaluminizing of carbon steels with a barrier component based on electrochemical nickel has not been practically studied and is only of a review nature in the literature. Therefore, there is scientific and practical interest in establishing the regularities of the formation of composition, structure, and determining the properties (heat resistance, microhardness) of multi-component coatings involving chromium and aluminum with a barrier component based on electrochemical nickel.

The aim of this work is to study the structure, phase and chemical compositions, as well as the protective properties of coatings on AISI 1045 steel obtained by combining electrochemical nickel plating with subsequent complex diffusion chromoaluminizing.

## 2. MATERIALS AND METHODS

Coatings were applied on AISI 1045 steel and to the same steel after electrochemical nickel plating from aqueous electrolytes. Nickel plating was performed in a nickel sulfate solution ( $\text{NiSO}_4 \cdot 7\text{H}_2\text{O}$ ), with sodium sulfate ( $\text{Na}_2\text{SO}_4$ ) and magnesium sulfate ( $\text{MgSO}_4$ ) added to increase electrical conductivity. The process was carried out at a constant current density of 3 A/dm<sup>2</sup> and a temperature of 40 °C.

Complex diffusion chromoaluminizing was conducted using a powder contact method in a saturating mixture with the following composition (wt. %): 90 (Cr) + 10 (Al) + 47 ( $\text{Al}_2\text{O}_3$ ) + 3 (activators). The activators consisted of a mixture of halides: 3 wt.%  $\text{NH}_4\text{Cl}$  + 1 wt.%  $\text{NiCl}_2$ . The process was performed in a sealed reaction chamber at a temperature of 1050 °C for 4 hours.

The phase composition of the coatings studied in this work was determined using a Rigaku Ultima IV diffractometer in Cu  $K\alpha$ -radiation ( $\lambda = 0.1541841$  nm). The Bragg-Brentano focusing scheme was used, which allows recording lines with reflection angles from 20 to 90° with step  $\Delta 2\theta = 0.04$  deg. The tube accelerating voltage was 40 kV, current strength was 40 mA, and exposure time ranged from 30 minutes to 3 hours. The X-ray diffraction patterns were interpreted, and the lattice periods of the obtained phases were determined using the PowderCell 2.4 software package according to the Rietveld method (complete profile analysis). The obtained diffractograms were compared with the reference diffractograms in the ICDD PDF-2 diffractogram database.

The coating and oxide microstructure were analyzed using a scanning electron microscope (MIRA 3, Tescan Co., Czech Republic). Chemical composition measurements were conducted using an energy-dispersive X-ray microanalyzer (Oxford X-Max 80) with an active crystal area of 80 mm<sup>2</sup> (INCA X-Max, Oxford Instruments, Abingdon-on-Thames, UK).

Local phase analysis was carried out at an accelerating voltage of 20 kV. The exposure time for chemical analysis was 30 seconds. Energy-dispersive X-ray spectrum indexing was performed using commercial INCA software (Oxford Instruments, Abingdon-on-Thames, UK). The content of Cr, Al, Fe, and Ni was determined based on the  $L\alpha$  line energy and  $K\alpha$  line energy values.

Additional metallographic studies were conducted using a MIM-7 optical microscope. To reveal the coating's microstructure, a 3 % nitric acid solution in ethyl alcohol was used.

Oxidation tests were conducted in a resistance furnace (LHT 01/17 D) capable of operating up to 1700 °C with airflow. The heating rate was 10 °C/min. Specimens were weighed before and after oxidation using AS R2 "Radwag" analytical scales with a precision of 0.0001 g.

Microhardness measurements were performed using a Vickers 432 SVD device with a diamond Vickers pyramid indenter having an angle of 136 degrees. A load of 0.3 N was applied, with an indentation time of 10 seconds, holding under load for 10 seconds, and unloading for 10 seconds. Hardness values were automatically calculated based on the diagonal lengths of the indentations.

## 3. RESULTS AND DISCUSSION

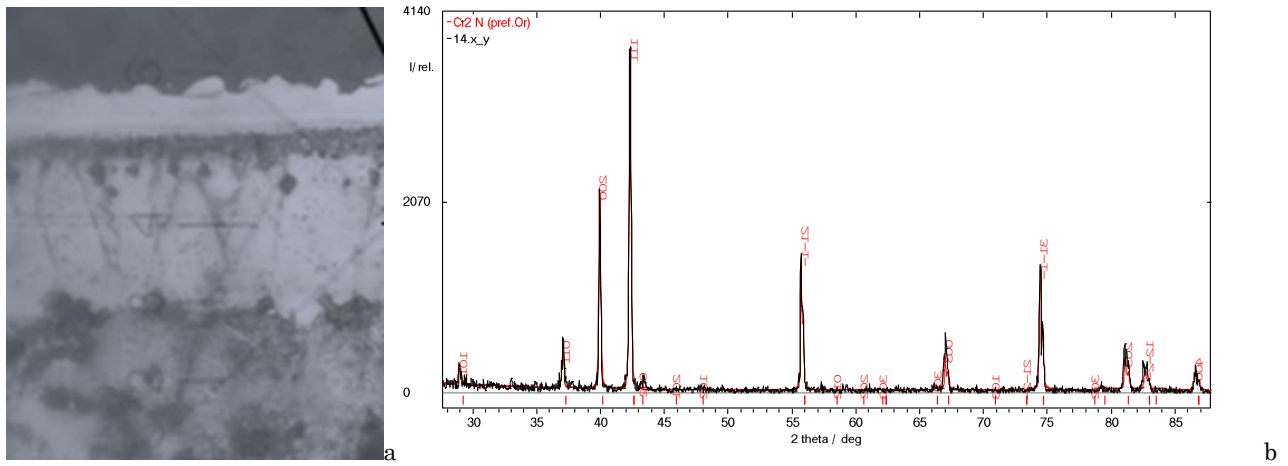
Microstructural analysis (Fig. 1a) revealed that the diffusion coating consists of four zones arranged parallel to the diffusion front. The outer layer has a bright, nearly white color and is uniformly distributed across the cross-section of the samples. No visible chipping or delamination of the surface zones was observed. The thickness of the obtained zone ranged from 11.5  $\mu\text{m}$  to 12.0  $\mu\text{m}$ .

It was established (Fig. 1b) that a surface layer based on chromium nitride  $\text{Cr}_2\text{N}$  (a: 4.8164 nm – 4.8166 nm, c: 4.4814 nm – 4.4816 nm) forms. The second zone differs slightly in terms of etching characteristics, with a thickness not exceeding 1.0  $\mu\text{m}$  – 1.5  $\mu\text{m}$ .

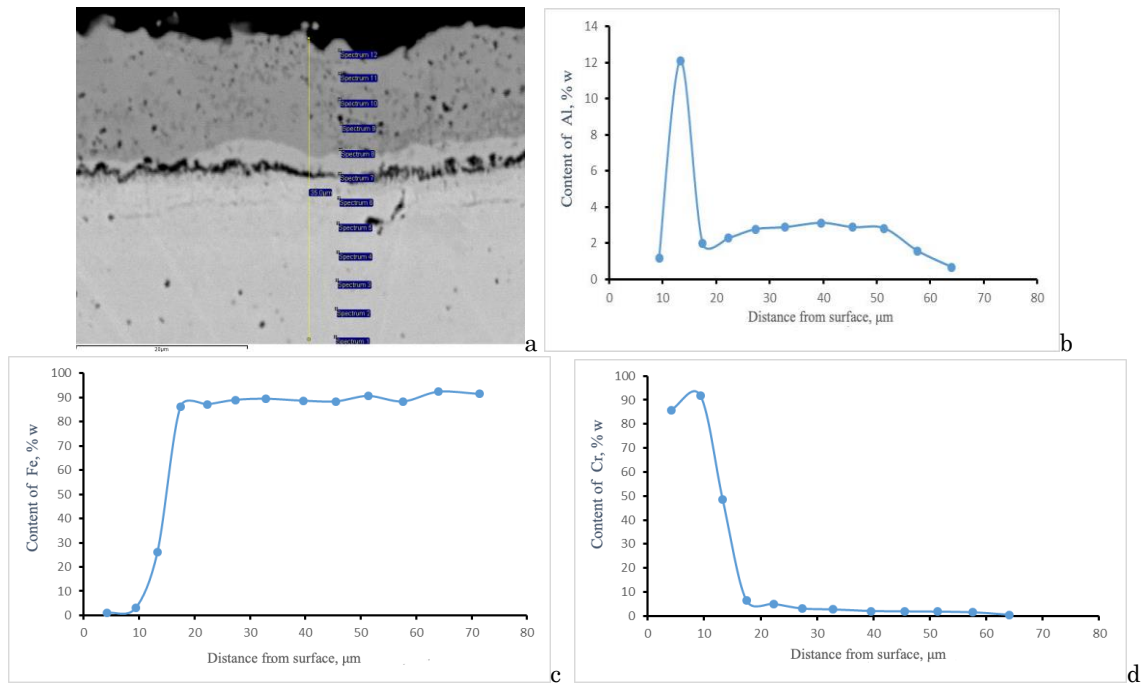
Next is a heterogeneous zone characterized by a dark, nearly black coloration. Small bright inclusions can be observed within this zone's structure. The thickness of this zone reaches 8.0  $\mu\text{m}$  – 9.5  $\mu\text{m}$ . Directly beneath the coating lies a light-colored transition zone with a characteristic columnar structure.

This zone likely forms due to the diffusion of Cr and Al into iron during the chemical-thermal treatment process. At the given treatment temperatures, when the solubility limit of chromium and aluminum in austenite is reached,  $\gamma\text{-Fe} - \alpha\text{-Fe}$  transformation occurs. The formation of the transition zone is accompanied by the displacement of the base boundaries, the formation of a ferrite zone, and characteristic columnar crystals. The thickness of the transition zone ranges from 50.0  $\mu\text{m}$  to 55.0  $\mu\text{m}$ .

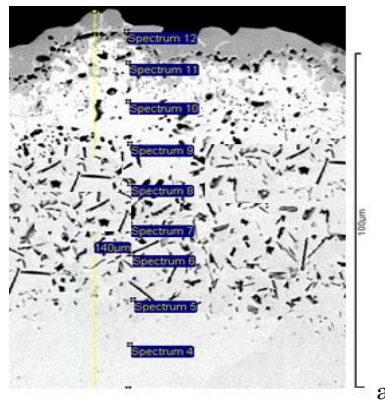
The microhardness of the first coating zone is quite high, reaching 16.0 GPa – 16.2 GPa. It was not possible to determine the microhardness of the second zone due to its small thickness. The microhardness of the third zone is 4.0 – 3.7 GPa, while the transition zone has a microhardness of 2.5 – 2.8 GPa.



**Fig. 1** – Microstructure (optics)  $\times 500$  (a), X-ray diffractogram (b) of the surface of AISI 1045 steel after complex diffusion chromoaluminizing (temperature – 1050 °C; time – 4 h); CuK $\alpha$  radiation, wavelength – 0.1541841 nm



**Fig. 2** – Microstructure, (SEM) (a), distribution of elements on the surface of the cross-sections of the surface of AISI 1045 steel after complex diffusion chromoaluminizing (temperature – 1050 °C; time – 4 h); (b, c, d)



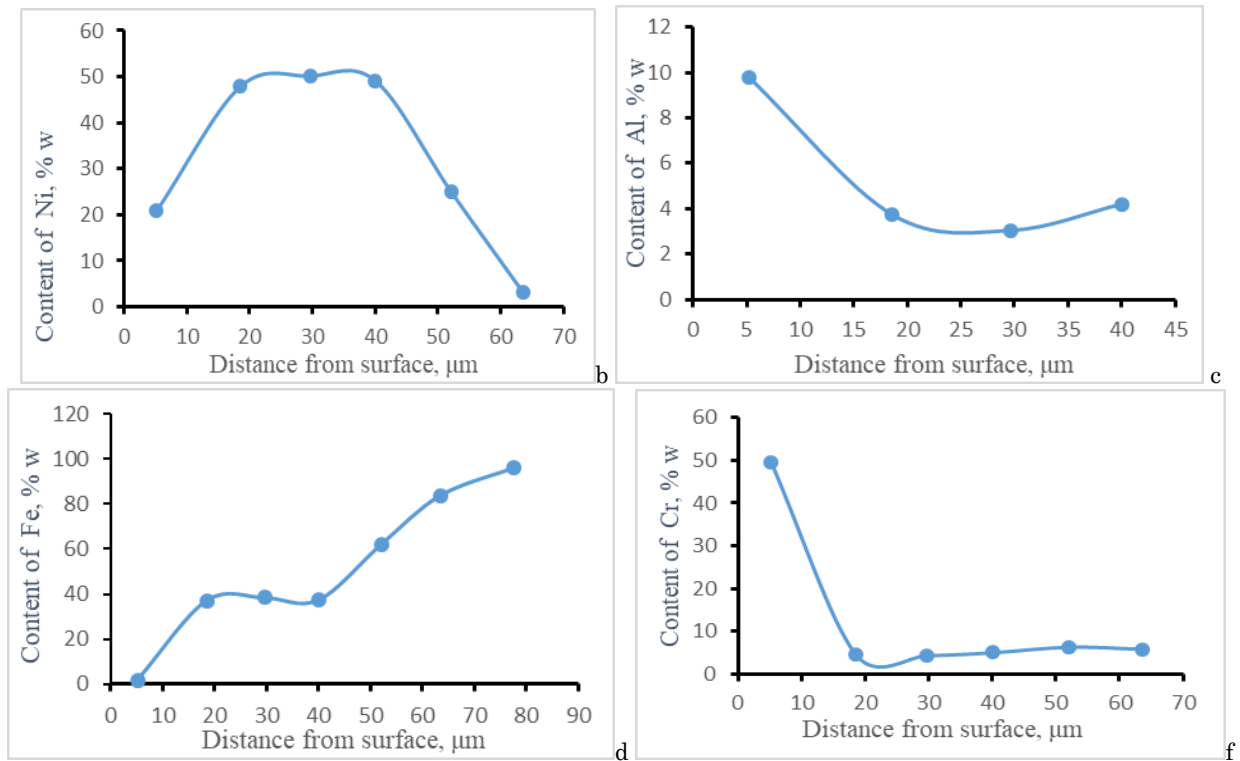


**Fig. 3** – Microstructure (a) and distribution of elements on the surface of the cross-sections of the surface of AISI 1045 steel (b-f) after nickel plating and complex diffusion chromoaluminizing (temperature – 1050 °C; time – 4 h)

\*Note: point 11 contains 7.95 wt. % N

It was established that a zone (Fig. 2, point 13) forms on the outer surface of the coatings, containing 85.79 wt. % Cr and 13.11 wt. % N. This zone was identified as the  $\text{Cr}_2\text{N}$  phase. The obtained data correlate well with the results of X-ray diffraction analysis and microhardness measurements (16.0 – 16.2 GPa). Notably, this phase contains almost no iron (up to 1.11 wt. %). The formation of this zone should contribute to an increase in the wear resistance of steel AISI 1045 [19].

Next is a zone with an increased chromium content of up to 91.81 wt. %, containing almost no other elements – 1.17 wt. % aluminum and 3.01 wt. % iron (Fig. 2, point 12).

Further, a zone corresponding to the Laves-phase-based  $\text{Cr}_2\text{Al}$  forms, containing 48.39 wt. % chromium, 12.1 wt. % aluminum, and 26.16 wt. % iron. The formation of this zone should enhance the heat resistance of AISI 1045 steel with chromoaluminizing coatings by promoting the formation of a dense, continuous oxide film  $(\text{Al,Cr})_2\text{O}_3$  during oxidation [6, 10].

As the coating progresses deeper, the chromium and aluminum contents sharply decrease to 6.61 wt. % – 5.05 wt. % and 3.99 wt. % – 2.29 wt. %, respectively (Fig. 2, point 10). In the zone based on the solid solution (Fig. 2, points 9 – 2), the aluminum content ranges from 2.78 wt. % to 1.58 wt. %, while the chromium content ranges from 3.12 wt. % to 1.52 wt. %. It is known [20] that with an aluminum content of 0.5–0.8 wt. %, a ferritic structure will be stabilized, which correlates well with the microstructural analysis data.

Coatings with a transition zone based on the  $\alpha\text{-Fe}(\text{Al,Cr})$  solid solution, having a hardness of

2.5–2.8 GPa, are unlikely to demonstrate high properties. Under conditions of contact interaction, the outer layer is expected to undergo deformation.

Before chromoaluminizing, a 20  $\mu\text{m}$  thick layer of electrochemical nickel was applied to some samples. It is known that nickel plating, aluminonickelizing, and chromonickelizing of metals and alloys through chemical-thermal treatment methods are generally considered impossible [21]. This is due to the absence of nickel subchlorides, which makes disproportionation reactions – the basis for gas-phase saturation methods – infeasible for nickel mass transfer to sample surfaces. The combination of two-step processing and the introduction of nickel-containing compounds ( $\text{NiCl}_2$ ) in the saturation mixture could present both scientific and practical significance as an innovative approach.

It was found that this stepwise treatment results in the formation of a fundamentally new type of coating. The obtained coatings were identified by microstructural analysis and micro-X-ray spectral analysis (Fig. 3). A heterogeneous coating was uniformly formed across the sample cross-sections. A gray-colored surface layer with inclusions of a lighter, almost white color was observed. The gray component corresponds to nearly pure chromium (99.3 wt. %). The light component contains 7.95 wt. % N, 20.82 wt. % Ni, 9.76 wt. % Al, 49.55 wt. % Cr, and almost no iron (up to 1.81 wt. %).

The light component was believed to correspond to solid solutions of Cr, Ni, and Al in Fe and N and could be generally represented by the formula  $(\text{Fe,Cr,Ni,Al})_x\text{N}$ . In these solutions, metals (nickel, chromium, aluminum) form substitution sublattices, while nitrogen forms

interstitial sublattices. The thickness of this layer was found to be between 10.0  $\mu\text{m}$  and 15.0  $\mu\text{m}$ .

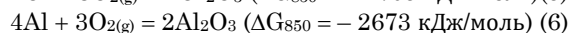
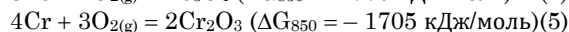
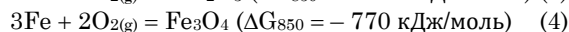
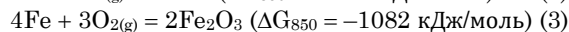
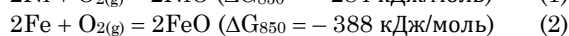
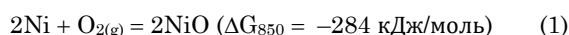
The next layer had a white color with dark, needle-like inclusions and a thickness of 65.0  $\mu\text{m}$  to 70.0  $\mu\text{m}$ . The base of this layer corresponds to a zone containing 50.13 wt. % nickel, 3.72 – 4.2 wt. % aluminum, 4.41 – 4.95 wt. % chromium, and 37.15 – 37.35 wt. % iron. According to the Fe-Ni-Cr phase diagram [22], such elemental concentrations result in the formation of a solid solution of chromium and nickel in  $\gamma\text{-Fe}$ . The formation of an austenitic structure with a high nickel content (in the range of 10 % to 40 % Ni) should positively influence resistance to stress corrosion cracking [23].

The needle-like inclusions were identified as a phase with a high oxygen content (up to 45.9 wt. %). These inclusions contained 37.36 wt. % aluminum, 4.7 wt. % chromium, with the remainder being iron. These inclusions were identified as complex spinel-type oxides involving chromium, aluminum, and iron. According to the theory of heat-resistant alloying [24], alloying elements that form double oxides are expected to have high protective properties. Such alloying elements must not lead to the formation of Fe-based compounds with a wüstite structure on the surface. Instead, they should form spinel-type oxides (double compounds, double oxides such as  $\text{FeCr}_2\text{O}_4$ ,  $\text{FeAl}_2\text{O}_4$ ,  $\text{NiFe}_2\text{O}_4$ , and  $\text{NiCr}_2\text{O}_4$ ) on the surface of metals and alloys.

As the coating progressed deeper, the nickel content gradually decreased, reaching 25.02 wt. % at a depth of 55 – 57  $\mu\text{m}$ , while the chromium content was 6.25 wt. %. No aluminum diffusion into the base matrix or the formation of a solid solution based on  $\alpha\text{-Fe}$  was observed.

It is well known that products made from carbon steels require strengthening heat treatment to form a stronger and harder structure beneath the coating and to prevent the indentation of protective layers during operation [25]. For AISI 1045, the recommended heat treatment involves normalization or full quenching followed by high tempering [26]. As a result of normalization and subsequent high tempering, a granular sorbite structure with optimal mechanical properties is formed. The normalization temperature for AISI 1045 is 850–900  $^\circ\text{C}$ . From an economic and technological standpoint, it is more appropriate to heat samples with coatings for normalization without using protective atmospheres. Therefore, studying the effect of heating to normalization temperatures on the structure and properties of coatings when processing in an air atmosphere is of undeniable interest.

During the analysis of the oxidation process, the most thermodynamically probable chemical reactions occurring during this process were identified. In our case, this involves the interaction of oxygen with iron and coating components (Cr, Al, Ni), which can be described by the following reaction equations:



According to the reaction equations in the oxidation process, the following oxide phases may form: NiO, FeO,  $\text{Fe}_2\text{O}_3$ ,  $\text{Fe}_3\text{O}_4$ , NiO,  $\text{Cr}_2\text{O}_3$ ,  $\text{Al}_2\text{O}_3$ . Thermodynamic calculations indicate that the formation of aluminum oxide is thermodynamically favorable, as the Gibbs free energy is the lowest compared to the other phases (equation 6). In terms of stability, the chromium oxide  $\text{Cr}_2\text{O}_3$ , iron oxide  $\text{Fe}_2\text{O}_3$ , and nickel oxide NiO follow. It should be noted that nickel oxide has the highest Gibbs energy, indicating its high stability when interacting with oxygen.

Oxidation was carried out at a temperature of 850  $^\circ\text{C}$  for 8 hours. The obtained data are presented in Fig. 4. It is shown that heat resistance increases: AISI 1045  $\rightarrow$  (Cr-Al)  $\rightarrow$  Ni(Cr-Al).

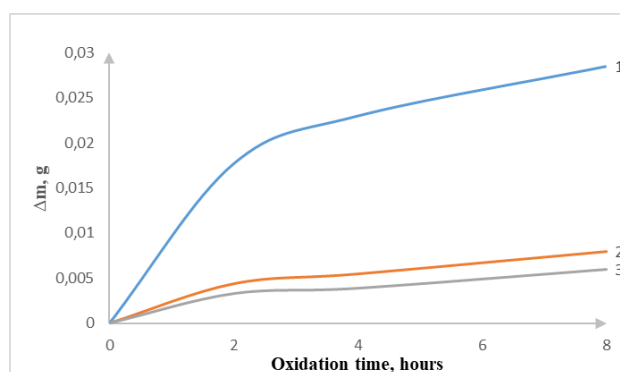


Fig. 4 – Oxidation kinetics of the initial AISI 1045 steel (1), AISI 1045 steel after diffusion chromoaluminizing (2), electrochemical nickel plating followed by diffusion chromoaluminizing (3), temperature 850  $^\circ\text{C}$ , duration 8 hours

It has been determined that after exposure to air for 8 hours at a temperature of 850  $^\circ\text{C}$ , a thick scale forms on the surface of the AISI 1045 steel samples, with a thickness of 160  $\mu\text{m}$  – 170  $\mu\text{m}$  (Fig. 5). On the surface, a layer based on  $\text{Fe}_3\text{O}_4$  is formed, beneath which is a thin layer of  $\text{Fe}_2\text{O}_3$ .

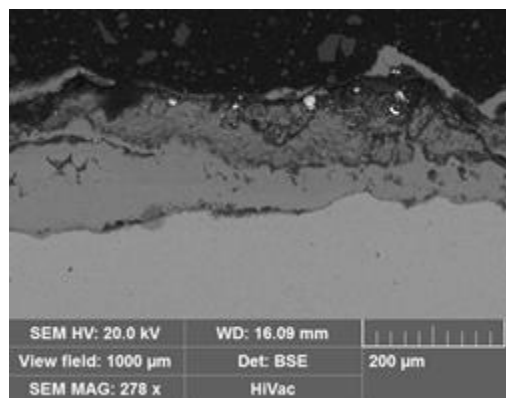
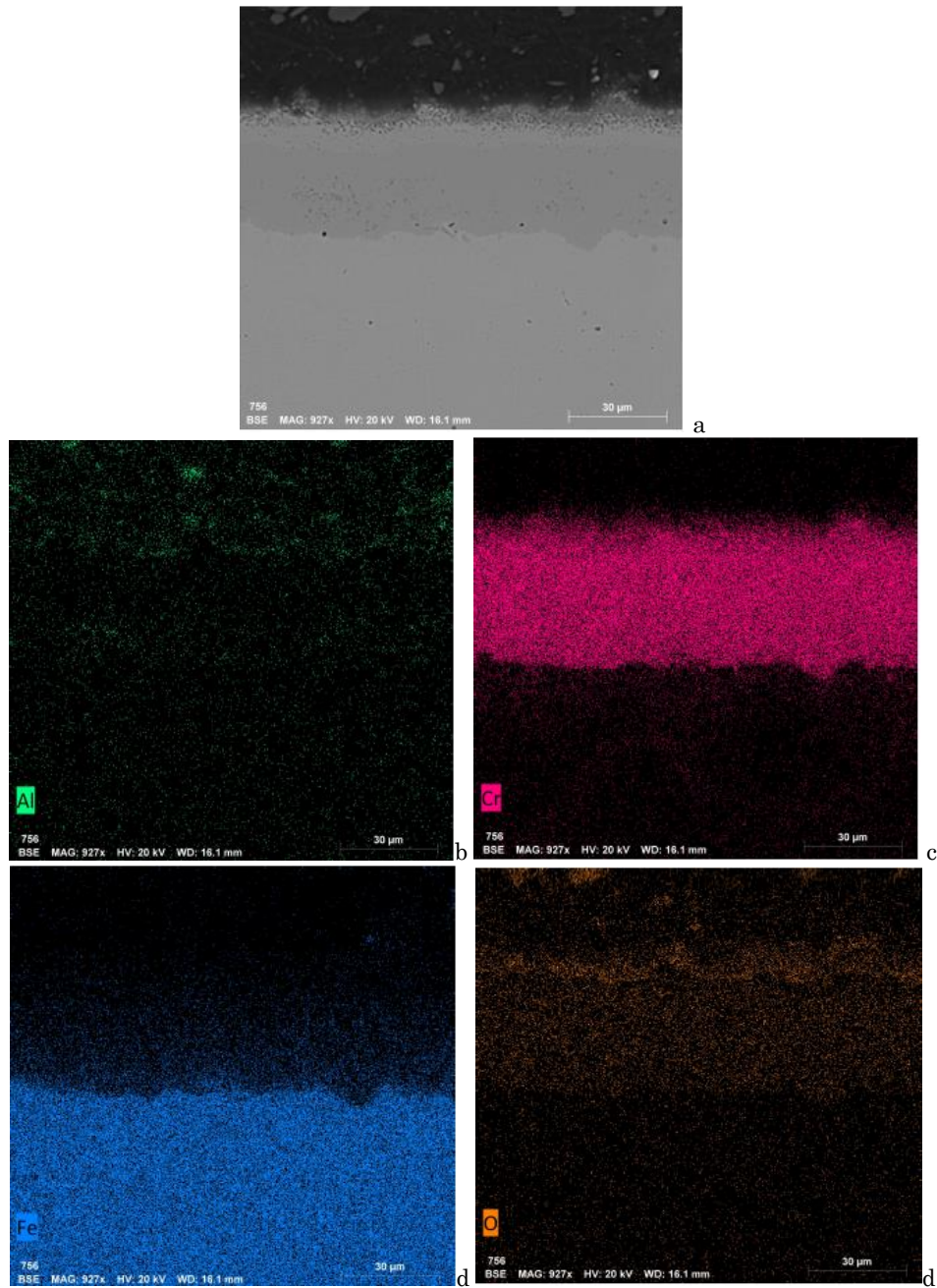
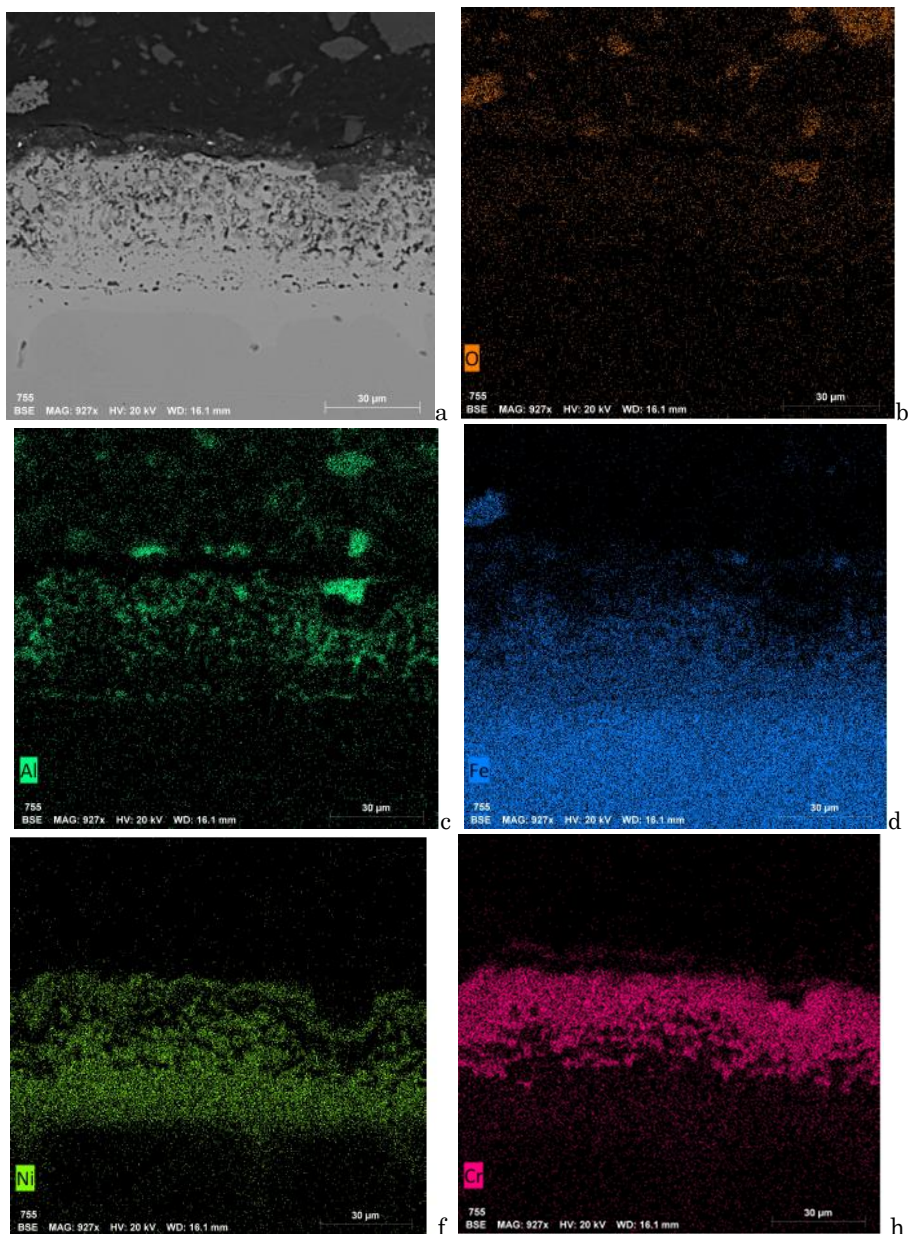


Fig. 5 – Microstructure of AISI 1045 steel after oxidation at 850  $^\circ\text{C}$  for 8 hours

The oxidation behavior of AISI 1045 steel with coatings of this type is different. It has been established (Fig. 6) that after exposure to air for 8 hours at a temperature of 850  $^\circ\text{C}$ , a zone with an increased content of aluminum and oxygen forms in the surface layer of the AISI 1045 steel samples with chromoaluminizing coatings. The migration of aluminum to the surface of



**Fig. 6** – Microstructure (a) and element distribution map (b-f) (characteristic X-ray emission in secondary electrons) across the surface plane of the AISI 1045 steel with a coating obtained by complex chromaluminizing after oxidation at 850 °C for 8 hours



**Fig. 7** – Microstructure (a) and element distribution map (b-h) (characteristic X-ray emission in secondary electrons) across the surface plane of the AISI 1045 steel with a coating obtained by galvanic nickel plating followed by complex chromoaluminizing after oxidation at 850 °C for 8 hours

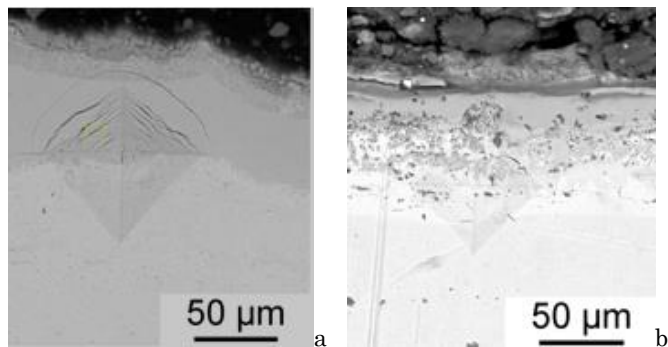


**Fig. 8** – Microstructure of the oxidized coating after microhardness measurement, load 0.3 N, a – AISI 1045 steel after chromoaluminizing, b – AISI 1045 steel after nickel plating followed by chromoaluminizing

the coating is likely related to its greater thermodynamic activity compared to chromium when interacting with oxygen, which aligns well with the thermodynamic calculations performed. The formed zone was identified as aluminum oxide  $\text{Al}_2\text{O}_3$ . The thickness of this layer is 2-3  $\mu\text{m}$ . It should be noted that the majority of the oxygen is concentrated in the surface layers of the coating. Beneath this layer is a zone with the maximum concentration of chromium, and the amount of oxygen in this layer decreases.

The formed layer was identified as chromium oxide  $\text{Cr}_2\text{O}_3$ . The chromium oxide layer is evenly distributed across the entire cross-section of the samples, and no visible defects were observed, making it promising in terms of heat resistance.

In the coatings obtained by nickel plating followed by chromoaluminizing (Fig. 7), the oxidation zone is confined to the surface layer with an increased content of aluminum and chromium, which was identified as  $(\text{Cr}, \text{Al})_2\text{O}_3$  oxide. According to the element distribution map, several characteristic zones of Ni, Cr, and Al can be distinguished, which correspond to the region that did not undergo oxidation and performs a barrier function.

The formation of a nickel-based barrier layer has affected the mechanical properties of the coating after oxidation (Fig. 8). In the case of oxidation of AISI 1045 steel with a chromoaluminizing coating, a scale of  $\text{Cr}_2\text{O}_3\text{-Al}_2\text{O}_3$  composition forms, which is brittle and, after loading, forms a series of cracks in the layer that propagate through a transgranular mechanism. The preliminary nickel plating stabilizes the austenitic structure, which enhances the plasticity and should positively affect the mechanical properties of the material during operation.

Thus, the formation of coatings on the surface of AISI 1045 steel significantly increases its resistance to oxidation by forming a dense scale on the surface. The introduction of Ni as an interlayer changes the oxidation mechanism and allows for the production of coatings with greater plasticity.

#### 4. CONCLUSIONS

1. It was established that after comprehensive chromoaluminizing of 45 steel in a saturating mixture (90 wt. % Cr, 10 wt. % Al, 47 wt. %  $\text{Al}_2\text{O}_3$ , 2 wt. %  $\text{NH}_4\text{Cl}$ , 1 wt. %  $\text{NiCl}_2$ ) at a temperature of 1050  $^\circ\text{C}$  for 4 hours, a diffusion coating with a total thickness ranging from 20.5  $\mu\text{m}$  to 23.0  $\mu\text{m}$  is formed on the surface. A transition zone based on the  $\text{Fe}\alpha$  solid solution is formed beneath the coating. This zone exhibits a characteristic columnar structure, with a thickness ranging from 50.0  $\mu\text{m}$  to 55.0  $\mu\text{m}$ .

2. The micro-X-ray spectroscopic analysis revealed that a zone is formed on the surface of the coatings, containing 85.79 wt. % of Cr and 13.11 wt. % of N. According to the results of X-ray structural analysis, this zone corresponds to chromium nitride  $\text{Cr}_2\text{N}$ . Further, a zone with an increased chromium content is found, reaching up to 95.82 wt. % of Cr. This zone almost contains no other elements – 1.17 wt. % of aluminum, and 3.01 wt. % of iron. Next, there is a zone cor-

responding to the phase based on the Laves phases  $\text{Cr}_2\text{Al}$ , which contains 48.39 wt. % of chromium and 12.1 wt. % of aluminum. The iron content in this zone is 26.16 wt. %. As we move deeper into the coating, the amounts of chromium and aluminum sharply decrease, comprising 6.61 wt. % and 5.05 wt. % of chromium, and 3.99 wt. % and 2.29 wt. % of aluminum, respectively. In the zone based on solid solution, the aluminum content ranges from 2.78 wt. % to 1.58 wt. %, and the chromium content ranges from 3.12 wt. % to 1.52 wt. %.

3. The microstructural analysis determined that the obtained coating consists of four zones. These zones are arranged parallel to the diffusion front. No visible chipping or delamination of the surface zones was observed. The microhardness of the surface zone of the coating is 16.2–16.0 GPa.

4. It has been established that a fundamentally new type of coating is formed with a total thickness of 35–45  $\mu\text{m}$  after the complex chromalithening of steel 45 with a previously applied 20  $\mu\text{m}$  thick nickel-based layer. The formation of a transition zone based on the  $\alpha\text{-Fe}$  solid solution was not observed in this case.

5. Microstructural and micro-X-ray spectroscopic analyses have shown that as a result of this two-stage treatment, a heterogeneous coating is formed on the surface of steel 45. A grey-colored layer forms on the surface, in which lighter grey inclusions are observed. According to the micro-X-ray spectroscopic analysis, the light component contains 7.95 % by weight of N, 9.76 % by weight of Al, 49.55 % by weight of Cr, 20.82 % by weight of Ni, and almost no iron. It is assumed that solid solutions of Cr, Ni, Al in Fe, and CrN were formed on the surface. The grey inclusions correspond to nearly pure chromium, containing 99.3 % by weight of the latter. Next, there is a white-colored layer with dark, needle-like inclusions. The base of this layer corresponds to a zone of compounds containing 3.72–4.2 % by weight of aluminum, 4.41–4.95 % by weight of chromium, 50.13 % by weight of nickel, and 37.15–37.35 % by weight of iron, corresponding to the solid solution of chromium and nickel in  $\gamma\text{-Fe}$ . The needle-like inclusions correspond to a phase with a higher oxygen content (up to 45.9 % by weight). The aluminum content in these inclusions is 37.36 % by weight, chromium is 4.7 % by weight, and the rest is iron. The obtained inclusions have been identified as complex spinel-type oxides involving chromium, aluminum, and iron. As we move deeper into the coating, the nickel content gradually decreases, and at a depth of 55–57  $\mu\text{m}$ , it is 25.02 % by weight, with chromium at 6.25 % by weight. No diffusion of aluminum into the matrix of the base or formation of a solid solution based on  $\alpha\text{-Fe}$  was observed.

6. It has been established that the coatings on the surface of steel 45 significantly enhance its oxidation resistance due to the formation of a dense scale on the surface. In coatings with a nickel-based layer, the oxidation zone is limited to the surface layer with an increased content of aluminum and chromium.



## REFERENCES

1. L. Von Fieandt, T. Larsson, E. Lindahl, O. Backe, M. Boman, *Surf. Coat. Technol.* **334**, 373 (2018).
2. S Kowalski, *Maint. Reliab.* **20**, 1 (2018).
3. T. Hovorun, A. Chornous, *Cryst. Res. Technol.* **41** No 5, 458 (2006).
4. Y.G. Chabak, V.I. Fedun, T.V. Pastukhova, et al., *Probl. At. Sci. Technol.* **110**, 97 (2017).
5. T. Loskutova, M. Hatala, I. Pogrebova, et al., *Coatings* **12**, 616 (2022).
6. G.S. Fox-Rabinovich, D.S. Wilkinson, S.C. Veldhuis, et al., *Intermetallics* **14**, 189 (2006).
7. O.M. Barabash, Y.V. Milman, D.V. Miracle, et al., *Intermetallics* **11**, 953 (2003).
8. M. Zhu, S. Achache, M.P. Motta, et al., *Coatings* **13**, 883 (2023).
9. P.C. Angelo, B. Ravisankar, *Introduction to Steels: Processing, Properties, and Applications* (CRC Press: 2021).
10. T. V. Loskutova, I. S. Pogrebova, V. G. Khyzhnyak, et al., *Mater. Today* **6**, 202 (2019).
11. L. Zhu, X. Wang, X. Ren, et al., *J. Eur. Ceram. Soc.* **42**, 921 (2022).
12. V.G. Khizhnyak, M.V. Arshuk, T.V. Loskutova, *Met. Sci. Heat Treat.* **58** No 3-4, 231 (2016).
13. Z. Cai, S. Liu, L. Xiao, et al., *Surf. Coat. Technol.* **324**, 182 (2017).
14. D. Monceau, B. Pieraggi, *Oxid. Met.* **50** No 5/6, 477 (1998).
15. Y. Qiao, T. Chen, X. Guo, *Corros. Commun.* **4**, 45 (2021).
16. Y. Qiao, X. Zhang, X. Guo, *Corros. Sci.* **196**, 110044 (2022).
17. Nasser Kanani, *Electroplating: Basic Principles, Processes and Practice* (Elsevier: 2004).
18. Nickel Institute. *Nickel Plating Handbook* (2023).
19. I. Pavlenko, J. Zajac, N. Kharchenko, et al., *Metals* **11** No 8, 115 (2021).
20. T. Narita, Y. Kato, T. Narita, et al, *High Temp. Corros. Mater.* **100**, 399 (2023).
21. G. Krauss, *Principles of Heat Treatment of Steel* (Metals Park, Ohio: American Society for Metals: 1980).
22. V. Raghavan, *J. Phase Equilib. Diffus.* **30**, 94 (2009).
23. P. Rodriguez, H.S. Khatak, J.B. Gnanamoorthy, *Bull. Mater. Sci.* **17**, 685 (1994).
24. P.I. Stoyev, S.V. Lytovchenko, I.O. Hirka, V.T. Hrytsyna, *Khimichna korozija ta zakhyst metaliv: navchal'nyy posibnyk* (Kh.: KhNU im. V. N. Karazina, 2019).
25. V. Loskutov, V. Khizhnyak, I. Pohrebova, *Carbide Coatings on Steels and Hard Alloys*; (Lileya: Ternopil, Ukraine: 1998).
26. Nestor Perez, *Materials Science: Theory and Engineering* (Textbook: 2024).

### Вплив електрохімічного нікелювання на структуру, склад та жаростійкість хромоалітованої сталі 45

Т.В. Лоскутова<sup>1,2</sup>, Я.А. Кононенко<sup>1</sup>, Н. Харченко<sup>3</sup>, О.П. Уманський<sup>4</sup>, Д.В. Ведель<sup>4</sup>, Т.П. Говорун<sup>3</sup>

<sup>1</sup> Національний технічний університет України «КПІ ім. І. Сікорського», 03056 Київ, Україна

<sup>2</sup> Університет Отто фон Геріке Магдебурга, 39106 Магдебург, Німеччина

<sup>3</sup> Сумський державний університет, 40007 Суми, Україна

<sup>4</sup> Інститут проблем матеріалознавства ім. І.М.Францевича НАН України, 03142 Київ, Україна

Досліджено процеси формування дифузійних покриттів на сталі 45 після двох методів насичення: дифузійного хромоалітування та комплексна двоетапна обробка (електрохімічного нікелювання та дифузійне хромоалітування). Нікелювання здійснювали в електролітах на основі сірчанокислового нікелю за температури 40 °С та щільності струму 3 А/дм<sup>2</sup>. Комплексне хромоалітування проводили порошковим методом при 1050 °С протягом 4 годин. Встановлено, що на поверхні формуються дифузійні покриття загальною товщиною від 20.5 мкм до 23.0 мкм із перехідною зоною на основі твердого розчину  $\alpha$ -Fe товщиною до 55 мкм. Мікрорентгеноспектральний аналіз показав наявність нітриду хрому Cr<sub>2</sub>N, а також зон з фазами Cr<sub>2</sub>Al та твердим розчином хрому й алюмінію. Отримане покриття складається з чотирьох зон. Мікротвердість поверхневої зони покриття 16.0 – 16.2 ГПа. Дифузійне хромоалітування зразків сталі 45 з шаром на основі нікелю товщиною 20 мкм реалізували при температурі 1050 °С впродовж 4 годин. Комплексна двоетапна обробка призводить до формування покриття товщиною 35 – 45 мкм. Показано, що формування захисних покриттів значно підвищує стійкість сталі 45 до окиснення завдяки утворенню щільної оксидної плівки. Визначено структуру оксидних включень, які містять хром, алюміній та залізо, що утворюють шпінельні фази. Двостадійний процес з попереднім нікелюванням забезпечив рівномірне розташування гетерогенних шарів без відшарувань. Додаткова попереднє нікелювання змінює механізм окислення та дозволяє отримати покриття, які мають більшу пластичність.

**Ключові слова:** Покриття, Комплексна дифузійна насиченість, Оксид.